

Crossover scaling from classical to non-classical critical behaviour

Sergio Caracciolo

*Scuola Normale Superiore and INFN – Sezione di Pisa
I-56100 Pisa, ITALIA*

Maria Serena Causo

*Höchstleistungsrechenzentrum (HLRZ)
Forschungszentrum Jülich
D-52425 Jülich, GERMANY*

Andrea Pelissetto

Paolo Rossi

Ettore Vicari

*Dipartimento di Fisica and INFN – Sezione di Pisa
Università degli Studi di Pisa
I-56100 Pisa, ITALIA*

Abstract

Interacting physical systems in the neighborhood of criticality (and massive continuum field theories) can often be characterized by just two physical scales: a (macroscopic) correlation length and a (microscopic) interaction range, related to the coupling and measured by the Ginzburg number G . A critical crossover limit can be defined when both scales become large while their ratio stays finite. The corresponding scaling functions are universal, and they are related to the standard field-theory renormalization-group functions. The critical crossover describes the unique flow from the Gaussian to the nonclassical fixed point.

Every physical situation of experimental relevance has at least two scales: one scale is intrinsic to the system, while the second one is related to experimental conditions. In Statistical Mechanics (SM) the correlation length ξ is related to experimental conditions (it depends on the temperature), while the interaction length (Ginzburg parameter) is intrinsic. The opposite is true in Quantum Field Theory (QFT): here the correlation length (inverse mass gap) is intrinsic, while the interaction scale (inverse momentum) depends on the experiment. Physical predictions are functions of ratios of these two scales and describe the crossover from the correlation-dominated (ξ/G or p/m large) to the interaction-dominated (ξ/G or p/m small) regime. In a properly defined limit they are universal and define the unique flow between two different fixed points.

In this discussion we will consider the crossover between the Gaussian point where mean-field predictions hold (interaction-dominated regime) to the standard Wilson-Fisher critical point (correlation-dominated regime).

Massive continuum field theory is the natural setting for a description of this critical crossover behavior, not only in QFT, where only two scales characterize (super)renormalizable theories, but also in SM, where in principle one might expect many scales (lattice spacing, geometry of interactions, ...) to play a role, and universality may be questioned. As we will discuss, critical crossover scaling exists and is universal when two scales become very large with respect to any other (microscopic) scale. Their ratio becomes the (universal) control parameter of the system, whose transition from 0 to ∞ describes the critical crossover.

In recent years there has been extensive work [1, 2, 3, 4, 5, 6, 7, 8, 9, 10, 11] aiming at the identification of the correct, theoretical and experimental, definition of the critical crossover limit. We give here a sketch of the argument for d -dimensional N -component vector spin models, but the notion may easily be extended to many other physical systems.

Let us start with the standard Landau-Ginzburg Hamiltonian on a d -dimensional lattice,

$$\begin{aligned} \mathcal{H} = & \sum_{i,j} \frac{1}{2} J(\vec{x}_i - \vec{x}_j) [\phi(\vec{x}_i) - \phi(\vec{x}_j)]^2 \\ & + \sum_i \left[\frac{1}{2} r \phi(\vec{x}_i)^2 + \frac{u}{4!} \phi(\vec{x}_i)^4 - h \phi(\vec{x}_i) \right], \end{aligned} \quad (1)$$

where $\phi(\vec{x}_i)$ are N -dimensional vectors. We will first consider the short-range case in which $J(\vec{x})$ is the standard nearest-neighbour coupling. For

this model the interaction scale is controlled by the coupling u and the relevant parameters are the (thermal) Ginzburg number G and its magnetic counterpart G_h defined by:

$$G = u^{2/(4-d)}, \quad G_h = u^{(d+2)/[2(4-d)]}. \quad (2)$$

Under a renormalization-group (RG) transformation G scales like the (reduced) temperature, while G_h scales as the magnetic field. For $t \equiv r - r_c \ll G$ and $h \ll G_h$ one observes the standard critical behaviour, while in the opposite case the behaviour is classical. The critical crossover limit corresponds to considering $t, h, u \rightarrow 0$ keeping $\tilde{t} = t/G$ and $\tilde{h} = h/G_h$ fixed. This limit is universal, i.e. independent of the detailed structure of the model: for Hamiltonians (1) the same behaviour is obtained as long as the interaction is short-ranged, i.e. for any $J(\vec{x})$ such that $\sum_x x^2 J(\vec{x}) < +\infty$. The crossover functions can be computed in the standard continuum ϕ^4 theory [3, 4, 5]. A dimensional analysis shows that (using the subtracted bare mass and removing the cutoff) finite results can be obtained directly in terms of the dimensionless variable $u/t^{2-d/2} = \tilde{t}^{d/2-2}$, and no further limiting procedure is required. It is important to observe that the critical crossover functions are related to the standard continuum RG functions if one expresses them in terms of the zero-momentum four-point renormalized coupling g . The crossover functions are well studied [3, 4, 5] in the fixed-dimension expansion when $d = 3$.

Let us now consider the long-range case. We assume that $J(\vec{x})$ has the following form

$$J(\vec{x}) = \begin{cases} J & \text{for } \vec{x} \in D, \\ 0 & \text{for } \vec{x} \notin D, \end{cases} \quad (3)$$

where D is a lattice domain characterized by some scale R . Explicitly we define R and the corresponding domain volume V_R by

$$V_R \equiv \sum_{\vec{x} \in D} 1, \quad R^2 \equiv \frac{1}{2d V_R} \sum_{\vec{x} \in D} x^2. \quad (4)$$

The shape of D is irrelevant for our purposes as long as $V_R \sim R^d$ for $R \rightarrow \infty$. The constant J defines the normalization of the fields. In our discussion it is useful to assume a long-range normalization, i.e. $J = 1/V_R$, since with this choice the limit $R \rightarrow \infty$ is well-defined. Notice that this is not the normalization that is commonly used discussing short-range models. Indeed,

in the latter case, one defines $J = R^{-2}/V_R$, so that the propagator behaves as k^2 for $k \rightarrow 0$. To understand the connection between the theory with long-range interactions and the short-range model let us perform an RG transformation [9]. Define new (“blocked”) coordinates $y_i = x_i/R$ and rescale the fields according to

$$\hat{\phi}(y_i) = R^{d/2}\phi(Ry_i), \quad \hat{h}(y_i) = R^{d/2}h(Ry_i). \quad (5)$$

The rescaled Hamiltonian becomes

$$\begin{aligned} \hat{\mathcal{H}} = & \sum_{i,j} \frac{1}{2} \hat{J}(\vec{y}_i - \vec{y}_j) \left[\hat{\phi}(\vec{y}_i) - \hat{\phi}(\vec{y}_j) \right]^2 \\ & + \sum_i \left[\frac{1}{2} r \hat{\phi}(\vec{y}_i)^2 + \frac{1}{4!} \frac{u}{R^d} \hat{\phi}(\vec{y}_i)^4 - \hat{h} \hat{\phi}(\vec{y}_i) \right], \end{aligned} \quad (6)$$

where now the coupling $\hat{J}(\vec{x})$ is of short-range type, i.e. independent of R . Being short-ranged, we can apply the previous arguments and define Ginzburg parameters:

$$G = (uR^{-d})^{2/(d-4)} = u^{2/(d-4)} R^{-2d/(4-d)}, \quad (7)$$

$$\begin{aligned} G_h &= R^{-d/2} (uR^{-d})^{(d+2)/[2(d-4)]} \\ &= u^{(d+2)/[2(d-4)]} R^{-3d/(4-d)}. \end{aligned} \quad (8)$$

Therefore, in the long-range model, the critical crossover limit can be defined as $R \rightarrow \infty$, $t, h \rightarrow 0$, with $\tilde{t} \equiv t/G$, $\tilde{h} \equiv t/G_h$ fixed. The variables that are kept fixed are the same, but a different mechanism is responsible for the change of the Ginzburg parameters: in short-range models we vary u keeping the range R fixed and finite, while here we keep the interaction strength u fixed and vary the range R . The important consequence of the argument presented above is that the critical crossover functions defined using the long-range Hamiltonian and the previous limiting procedure agree with those computed in the short-range model, apart from trivial rescalings.

Let us give a few examples. Let us introduce magnetic susceptibility, correlation length and magnetization in the usual way:

$$\chi = \sum_x \langle \phi_0 \cdot \phi_x \rangle, \quad (9)$$

$$\xi^2 = \frac{1}{2d\chi} \sum_x x^2 \langle \phi_0 \cdot \phi_x \rangle, \quad (10)$$

$$M = \langle \phi_0 \rangle. \quad (11)$$

Then one can show that in the limit $t \rightarrow 0$, $G, G_h \rightarrow 0$ with \tilde{t} and \tilde{h} fixed the following rescaled quantities have a finite limit:

$$\tilde{\chi} \equiv \chi G \rightarrow F_\chi(\tilde{t}, \tilde{h}), \quad (12)$$

$$\tilde{\xi}^2 \equiv R^{-2} \xi^2 G \rightarrow F_{\xi^2}(\tilde{t}, \tilde{h}), \quad (13)$$

$$\tilde{M} \equiv MG/G_h \rightarrow F_M(\tilde{t}, \tilde{h}), \quad (14)$$

where $F_\chi(\tilde{t}, \tilde{h})$, $F_{\xi^2}(\tilde{t}, \tilde{h})$, and $F_M(\tilde{t}, \tilde{h})$ are universal apart from a rescaling of \tilde{t} and \tilde{h} and of the functions themselves. Comparison with experimental data is usually performed introducing effective exponents. For instance, for $\tilde{h} = 0$, we can define

$$\gamma_{\text{eff}}(\tilde{t}) = -\tilde{t} \frac{d}{d\tilde{t}} \log F_\chi(\tilde{t}, 0), \quad (15)$$

$$\nu_{\text{eff}}(\tilde{t}) = -\frac{\tilde{t}}{2} \frac{d}{d\tilde{t}} \log F_{\xi^2}(\tilde{t}, 0). \quad (16)$$

These functions can be related to the standard RG functions if one expresses them in terms of the zero-momentum four-point coupling g . In the high-temperature phase one finds for instance (cf. Ref. [4])

$$\frac{\gamma_{\text{eff}}(g)}{\nu_{\text{eff}}(g)} = \frac{\gamma(g)}{\nu(g)}, \quad (17)$$

$$\nu(g)\beta(g) \frac{d\gamma_{\text{eff}}}{dg} = \gamma(g) - \gamma_{\text{eff}}(g), \quad (18)$$

where $\gamma(g)$, $\nu(g)$, and $\beta(g)$ are the standard RG functions. These effective exponents interpolate between the classical and the non-classical value. As an example, in Fig. 1, we report the graph of $\gamma_{\text{eff}}(\tilde{t})$ in the high- and low-temperature phase for the Ising model (the computation has been done using the results of Refs. [3, 4, 5]). These curves are in good agreement with numerical results for the long-range Ising model [12], even for very small values of R , i.e. for interactions extending over a few lattice spacings.

The ideas we have presented here can be explicitly checked in the large- N limit. All the crossover functions can be computed in the whole (t, h) -plane for $2 < d < 4$ and universality (model independence) can be explicitly checked. For instance for the effective exponents defined in Eqs. (15) and (16) one finds in three dimensions

$$\gamma_{\text{eff}}(\tilde{t}) = 2\nu_{\text{eff}}(\tilde{t}) = 1 + (1 + c_\gamma \tilde{t})^{-1/2}, \quad (19)$$

where c_γ is a non-universal constant.

One can also study the corrections to the leading universal behaviour. If R is chosen as in Eq. (4), one verifies that the corrections to the universal crossover functions scale as $1/R^d$ (for generic choices of scale one would observe instead $1/R$ -corrections).

The discussion of these non-universal effects can be extended to all values of N considering a perturbative expansion around the mean-field solution. Consider for instance the long-range Ising model

$$\mathcal{H} = -\frac{N\beta}{2} \sum_{i,j} J(\vec{x}_i - \vec{x}_j) s(\vec{x}_i) \cdot s(\vec{x}_j), \quad (20)$$

where $J(\vec{x})$ is defined in Eq. (3). For $N = 1$ and for a particular choice of D this is the model that has been studied in Refs. [8, 9, 12]. Computing the corrections to mean field allows us to determine the corrections to $\beta_c(R)$ for $R \rightarrow \infty$ for the Hamiltonian (20). One finds for $d > 2$

$$\beta_c(R) = \int \frac{d^d k}{(2\pi)^d} \frac{1}{\Pi(k)} \quad (21)$$

with corrections of order R^{-2d} (multiplicative logarithms appear for some special values of d , for instance for $d = 3$). Here

$$\Pi(k) = \frac{1}{V_R} \sum_{x \in D} (1 - e^{ikx}), \quad (22)$$

and the integral is extended over the first Brillouin zone. Expanding the integral in powers of R one finds

$$\beta_c(R) = 1 + \frac{\alpha}{R^d} + \dots \quad (23)$$

where α depends on the precise definition of the domain D . In two dimensions there are logarithmic corrections and one finds

$$\beta_c(R) = 1 + \frac{1}{4\pi R^2} \log R^2 + O(R^{-2}). \quad (24)$$

By considering the mean-field limit one can also relate the non-universal constants that appear in the definition of the crossover scaling functions. To give an example, consider $\tilde{\chi}$ for $\tilde{h} = 0$. The function $F_\chi(\tilde{t}, 0)$ can be computed

in perturbation theory, cf. Ref. [4], obtaining a function $F_\chi^{\text{sr}}(\tilde{t})$. On the other hand, if one considers the model (20) one obtains a different $F_\chi^{\text{lr}}(\tilde{t})$. As we explained above we should have

$$F_\chi^{\text{lr}}(\tilde{t}) = a_\chi F_\chi^{\text{sr}}(b\tilde{t}) . \quad (25)$$

The analysis of the mean-field limit provides exact expressions for a_χ , which depends on the observable, and b , which depends only on the model.

Finally we want to discuss the crossover scaling limit for models that have $\beta_c = +\infty$. This is the case of the two-dimensional N -vector model with $N \geq 3$. For these theories define

$$\hat{t} \equiv R^2 \left(1 + \frac{1}{4\pi R^2} \log R^2 - \beta \right) \quad (26)$$

and consider the limit $R \rightarrow \infty$ with \hat{t} fixed. One finds that the limits defined in Eqs. (12) and (13) still exist and define crossover functions of \hat{t} . For $\hat{t} \rightarrow +\infty$ these functions show mean-field behaviour, while standard asymptotic scaling is observed for $\hat{t} \rightarrow -\infty$. Notice that one can use \hat{t} as a variable instead of \tilde{t} also when β_c is finite. In this case, however, nothing new is obtained, since $\hat{t} - \tilde{t}$ is simply a constant for $R \rightarrow \infty$.

The model with Hamiltonian (20) can be studied in the limit $N \rightarrow 0$. In this case it can be rewritten in terms of self-avoiding walks (SAWs) [13] with long-range jumps. To be explicit, we define an n -step SAW with range R as a sequence of lattice points $\{\omega_0, \dots, \omega_n\}$ with $\omega_0 = (0, 0, 0)$ and $\omega_{j+1} \in D_R(\omega_j)$, such that $\omega_i \neq \omega_j$ for all $i \neq j$. Then, if $c_{n,R}(x)$ is the number of n -step SAWs with range R going from 0 to x , we indicate with $c_{n,R}$ the total number of n -step walks and with $E_{n,R}^2$ the mean square end-to-end distance. They are defined as:

$$c_{n,R} = \sum_x c_{n,R}(x), \quad (27)$$

$$E_{n,R}^2 = \frac{1}{c_{n,R}} \sum_x x^2 c_{n,R}(x). \quad (28)$$

One can then prove that

$$\lim_{N \rightarrow 0} \chi(\beta) = \sum_{n=0}^{\infty} \hat{\beta}^n c_{n,R}, \quad (29)$$

$$\lim_{N \rightarrow 0} \xi^2(\beta) \chi(\beta) = \frac{1}{2d} \sum_{n=0}^{\infty} \hat{\beta}^n c_{n,R} E_{n,R}^2. \quad (30)$$

where $\hat{\beta} = \beta/V_R$ and χ and ξ^2 are defined in the model (20).

The crossover limit is trivially defined remembering that n is the dual variable (in the sense of Laplace transforms) of t . Therefore we should study the limit $n \rightarrow \infty$, $R \rightarrow \infty$ with $\tilde{n} \equiv nR^{-2d/(4-d)}$ fixed. From Eqs. (12) and (13) we obtain that the following limits exist:

$$\tilde{c}_{n,R} \equiv c_{n,R} \beta_c(R)^n \rightarrow g_c(\tilde{n}), \quad (31)$$

$$\tilde{E}_{n,R}^2 \equiv E_{n,R}^2 R^{-8/(4-d)} \rightarrow g_E(\tilde{n}), \quad (32)$$

where the functions $g_c(\tilde{n})$ and $g_E(\tilde{n})$ are related by a Laplace transform to $F_\chi(\tilde{t}, 0)$ and $F_{\xi^2}(\tilde{t}, 0)$. Explicitly

$$F_\chi(t, 0) = \int_0^\infty du g_c(u) e^{-ut}, \quad (33)$$

$$F_{\xi^2}(t, 0) F_\chi(t, 0) = \frac{1}{2d} \int_0^\infty du g_c(u) g_E(u) e^{-ut}. \quad (34)$$

Using perturbation theory it is possible to derive predictions for E_n^2 and c_n . For E_n^2 we can write

$$g_{E,PT}(\tilde{n}) = a_E \tilde{n} h_E(z), \quad (35)$$

where $z = (\tilde{n}/l)^{1/2}$. The function $h_E(z)$ has been computed in perturbation theory to six-loop order [14]. Resumming the series with a Borel-Leroy transform one finds that a very good approximation is provided by [15]

$$h_E(z) = (1 + 7.6118z + 12.05135z^2)^{0.175166}. \quad (36)$$

Comparison with a detailed Monte Carlo simulation for the Domb-Joyce model indicates [15] that this simple expression differs from the exact result by less than 0.02% for $z < 2$.

The constants a_E and l appearing in Eq. (35) are non universal. For our specific model they are given by

$$a_E = 6, \quad l = (4\pi)^3. \quad (37)$$

We have performed [16] an extensive simulation of this model of long-range SAWs generating walks of length up to $N \approx 7 \cdot 10^4$. The domain D was chosen as follows:

$$D = \left\{ x : \sum_i |x_i| \leq \rho \right\}. \quad (38)$$

In the simulation we varied ρ between 2 and 12. Let us describe the results for the end-to-end distance. Analogous results can be obtained for $c_{n,R}$.

In Fig. 2 we report our results for $\tilde{E}_{n,R}^2$ together with the perturbative prediction $g_{E,PT}(\tilde{n})$ defined in Eqs. (35,36). The agreement is very good although one can see clearly the presence of corrections to scaling. In order to see better the discrepancies between the numerical data and the theoretical prediction we report in Fig. 3 the ratio $\tilde{E}_{n,R}^2/g_{E,PT}(\tilde{n})$. In this plot the corrections to scaling are clearly visible: points with different R fall on different curves that converge to 1 as expected. For $\rho = 12$, the deviations are less than 0.2%. It is interesting to observe that the corrections change sign with \tilde{n} . For $\tilde{n} \lesssim 2 \cdot 10^2$, the corrections are negative, while in the opposite case they are positive.

The corrections to scaling are expected¹ to scale as R^{-d} . To check this behaviour let us consider

$$\Delta_{E;n,R} \equiv \left[\tilde{E}_{n,R}^2/g_{E,PT}(\tilde{n}) - 1 \right] R^3. \quad (39)$$

The plot of $\Delta_{E;n,R}$ is reported in Fig. 4. A good scaling behaviour is observed confirming the theoretical prediction for the corrections. This nice scaling indicates also that the approximation (36) can be considered practically exact at our level of precision.

We have also defined an effective exponent ν_{eff}

$$\nu_{\text{eff}} = \frac{1}{2 \log 2} \log \left(\frac{E_{2n,R}^2}{E_{n,R}^2} \right). \quad (40)$$

It is reported in Fig. 5. It shows the expected crossover behaviour between the mean-field value $\nu = 1/2$ and the self-avoiding walk value $\nu = 0.58758(7)$ [15].

References

- [1] M. E. Fisher, Phys. Rev. Lett. **57**, 1911 (1986).
- [2] M. A. Anisimov, A. A. Povodyrev, V. D. Kulikov, and J. V. Sengers, Phys. Rev. Lett. **75**, 3146 (1995).

¹This behaviour should be observed only for quantities that are defined using R as scale. If we were considering for instance $E_{n,R}^2 \rho^{-8/(4-d)}$ we would of course obtain the same universal limiting curve, but now with corrections of order $1/\rho$.

- [3] C. Bagnuls and C. Bervillier, J. Phys. Lett. (Paris) **45**, L-95 (1984).
- [4] C. Bagnuls and C. Bervillier, Phys. Rev. **B 32**, 7209 (1985).
- [5] C. Bagnuls, C. Bervillier, D. I. Meiron, and B. G. Nickel, Phys. Rev. **B 35**, 3585 (1987).
- [6] M. A. Anisimov, S. B. Kiselev, J. V. Sengers and S. Tang, Physica **A 188**, 487 (1992).
- [7] M. Y. Belyakov and S. B. Kiselev, Physica **A 190**, 75 (1992).
- [8] E. Luijten, H. W. J. Blöte and K. Binder, Phys. Rev. **E 54**, 4626 (1996).
- [9] E. Luijten, H. W. J. Blöte and K. Binder, Phys. Rev. Lett. **79**, 561 (1997); Phys. Rev. **E 56**, 6540 (1997).
- [10] K. K. Mon and K. Binder, Phys. Rev. **E 48**, 2498 (1993).
- [11] A. Pelissetto, P. Rossi, and E. Vicari, `cond-mat/9804264` to appear in Phys. Rev. **E**.
- [12] E. Luijten and K. Binder, to appear in Phys. Rev. **E58** (Rap. Comm.) (1998).
- [13] M. Daoud *et al*, Macromolecules **8**, 804 (1975).
- [14] M. Muthukumar and B. G. Nickel, J. Chem. Phys. **80**, 5839 (1984); **86**, 460 (1987).
- [15] P. Belohorec and B. G. Nickel, Guelph report (September 1997).
- [16] S. Caracciolo, M. S. Causo, A. Pelissetto, P. Rossi, and E. Vicari, in preparation.

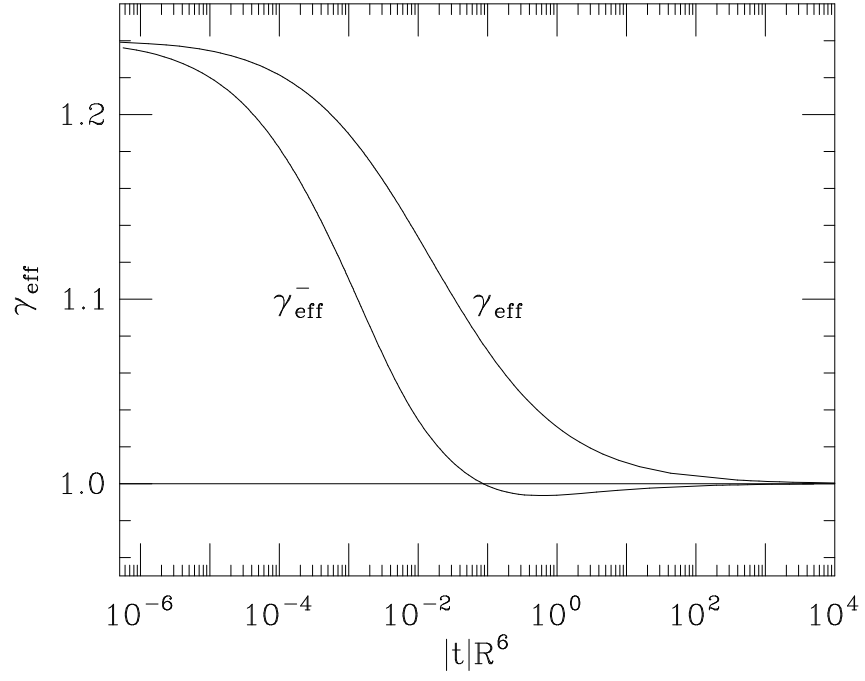


Figure 1: Effective susceptibility exponent as a function of \tilde{t} for the high- (γ_{eff}) and low- (γ_{eff}^-) temperature phase of the three-dimensional Ising model.

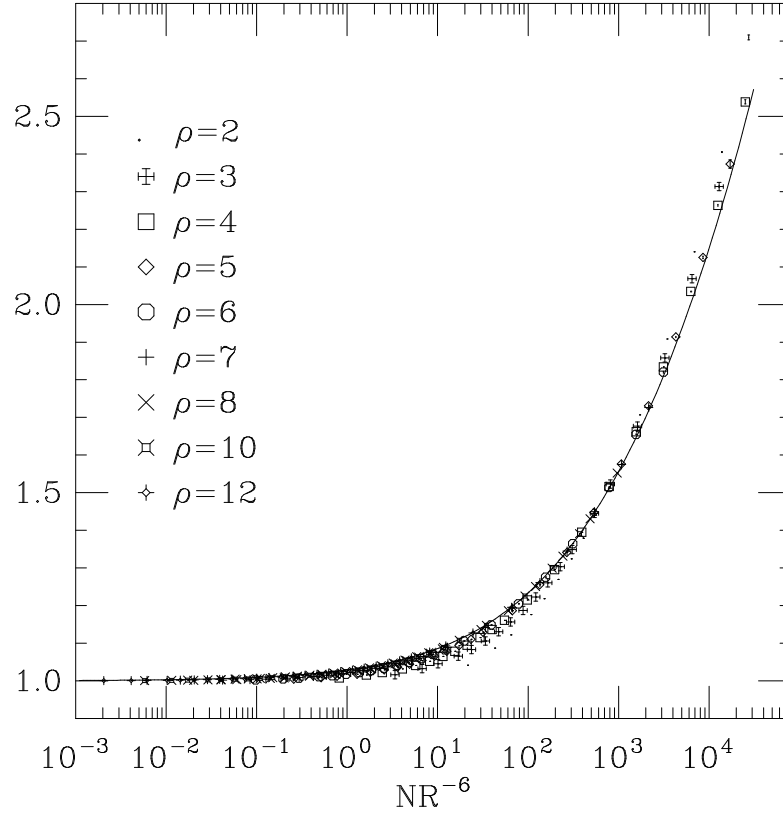


Figure 2: Results for $\tilde{E}_R^2/(6\tilde{n})$. The solid line is the theoretical prediction (35), (36).

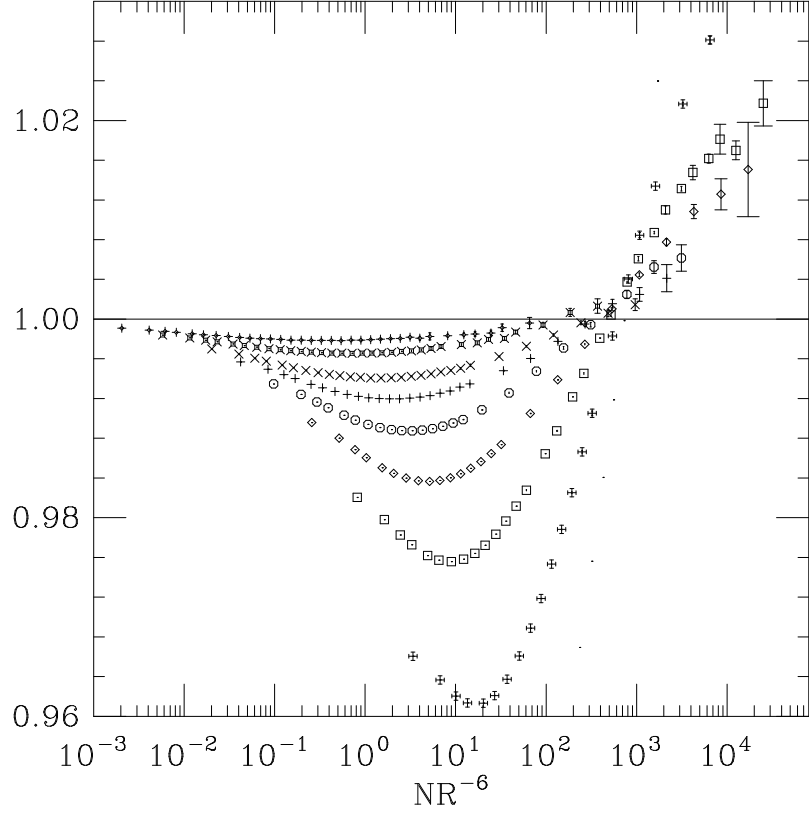


Figure 3: Results for $\tilde{E}_R^2 / g_{E,PT}(\tilde{n})$. We use the same symbols as in Fig. 2.

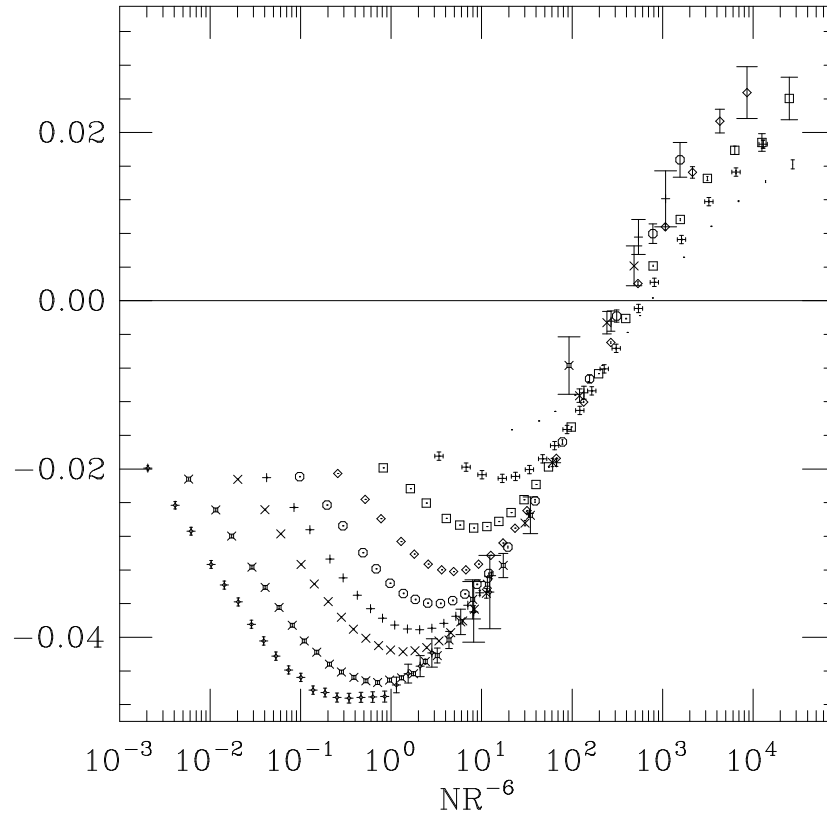


Figure 4: Results for $\Delta_{E;n,R}$. We use the same symbols as in Fig. 2.

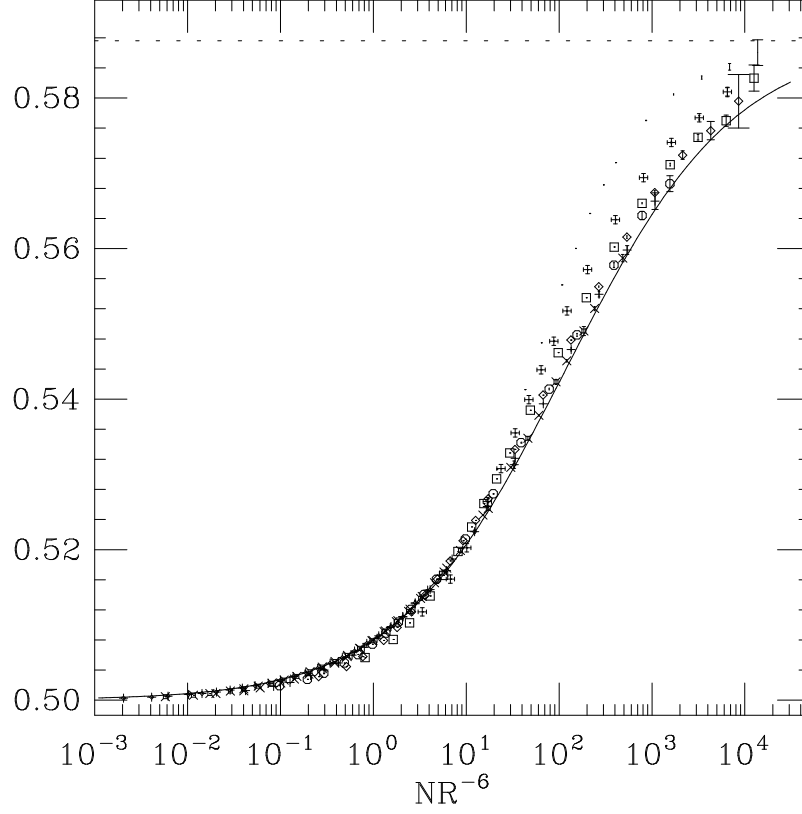


Figure 5: Results for ν_{eff} . We use the same symbols as in Fig. 2. The dashed line is the self-avoiding walk value $\nu = 0.58758(7)$. The solid line is the theoretical prediction.